Massive MIMO-enabled HetNets with Full Duplex Small Cells

Sunila Akbar*, Yansha Deng*, Arumugam Nallanathan†, Maged Elkashlan†, and George K. Karagiannidis‡
* Department of Informatics, King's College London, London, UK
† School of Electronic Engineering and Computer Science, Queen Mary University of London, London, UK
‡ Department of Electrical and Computer Engineering, Aristotle University of Thessaloniki, Thessaloniki, Greece

***Abstract*—Massive multiple input multiple output (MIMO) and full duplex (FD) communication are being considered as potential candidates for the spectrum efficient 5G wireless networks. In this paper, we develop a tractable model for downlink (DL) and uplink (UL) transmission in K-tier heterogeneous cellular networks (HCNs) with massive MIMO macrocells and full duplex (FD) small cells for spectrum efficiency. In the considered HCNs, the performance of the mobile user (MU) is limited by several sources of interference, specifically due to FD nature of small cell base stations (SBSs). A stochastic geometry based model of the proposed HCNs is provided which allows to derive the DL and UL rate coverage probabilities of such a system. Monte Carlo simulations confirm the accuracy of the analytical results, while numerical results reveal that equipping large number of MIMO antennas at macro base stations (MBSs) enhances the DL rate coverage probability of a random MU in HCNs. The results show that to achieve the maximum joint DL and UL performance gain in HCNs with FD small cells, both SBSs' density and SBSs' transmit power should be optimized. Moreover, the UL performance can be improved by decreasing the SBSs receivers sensitivity and increasing the UL power control factor.**

I. Introduction

The emerging fifth-generation (5G) wireless communication system targets higher data rates to support exponential increase in wireless data transmissions [1]. Massive multiple input multiple output (MIMO) and heterogeneous cellular networks (HCNs) are the key strategies towards meeting this challenge [1]–[4]. More specifically, HCNs are proposed to boost the network capacity through the dense deployment of small cell base stations (SBSs) [5] and massive MIMO enables fine-grained beamforming to each mobile user (MU) that brings high throughput data transmission [6].

Recently, increasing research has been conducted on full-duplex (FD) communication, which allows transmitting and receiving data simultaneously and within the same frequency band [7]. In theory, FD data transmission is capable of doubling the spectral efficiency of half-duplex (HD) system. Until now, FD has been hard to realize in practice due to the residual self-interference (SI). Fortunately, the recent advances towards SI cancellation, such as antenna separation schemes [8] and beamforming-based techniques [9] have demonstrated the feasibility of FD transmission for short to medium range wireless communications. The low transmit power of SBSs makes them attractive choice for FD operation since the SI at SBSs is more manageable compared to that at the high power macrocell base stations (MBSs).

The FD transmission in cellular networks has been studied in [10]–[16]. In [10], the area spectral efficiency (ASE) was derived for the small cell networks with FD communication and the SI was shown to be dominant compared with the aggregate interference. The work in [17] proposed in-band α-duplex scheme in multi-cell networks with FD operation in each cell, which allows a partial overlap between downlink (DL) and uplink (UL) frequency bands. Their results demonstrated that the overlap parameter α can be optimized to achieve maximum FD gain. The recent work in [11] presented the impact of FD cells on the area spectral efficiency vs. coverage trade-off of the system, however, this work only focused on the small cell network. In [12], the performance of a massive MIMO-enabled wireless backhaul network is evaluated, where each SBS can be configured either in-band or out-of-band FD backhaul mode. It is shown in [13] that making different tiers operate in different duplex modes in heterogeneous networks can enhance the network throughput. The cell association problem in multi-tier in-band FD networks was addressed in [14]. In [15], FD was used for device to device (D2D) communications to increase the throughput and reduce delay of video caching in cellular systems. In more recent work [16], the performance of two-tier interference-coordinated HCNs with FD small cells is investigated.

The aforementioned literature laid a solid foundation for the feasibility of FD communication in cellular networks. Inspired by the fact in [13] that making different tiers operate in different duplex modes in heterogeneous networks enhances the network throughput, in our work, we focus on HCNs, where only small cells operate in FD mode, whereas the macrocells operate in HD mode. However, we note that increasing the proportion of FD SBSs enhances the ASE of the network at the cost of coverage reduction [11]. To compensate this cost, a simple solution is to employ massive MIMO antennas at the MBSs that boost coverage [18]. The proposed network is analyzed by using tools from stochastic geometry, which provides tractable yet accurate analytical results in HCNs, such as our recent works on wireless powered HCNs [19], [20]. The main contribution of our work can be summarized as follows:

- We model K-tier HCNs composed of massive MIMO MBSs and FD SBSs with distance-proportional fractional

power control in the UL. We derive the analytical expressions for the DL and the UL rate coverage probabilities of the macrocell MU and small cell MU, and the UL rate coverage probability of the small cell MU based on stochastic geometry.

- We present that, the increase in number of antennas at the MBSs provides improved DL rate coverage probability. Moreover, the number of SBSs and the SBSs transmit power can be tuned in order to achieve maximum joint DL and UL performance gain. Moreover, we demonstrate that the distance-proportional fractional power control can be tuned to achieve a desirable performance in both DL and UL.

II. System Description

We consider K-tier HCNs, where the MBSs and the SBSs are spatially located in $\mathbb{R}^2$, following the homogeneous Poisson point process (HPPP), $\Phi_{b^{\mathrm{M}}}$ and Φ_{b^k} with intensity $\lambda_{b^{\mathrm{M}}}$ and λ_{b^k} $(k = 2, \cdots, K)$, respectively. We consider massive MIMO at the MBSs, where each MBS is equipped with N antennas, serving U_{M} MUs ($0 < U_{\mathrm{M}} \ll N$), and operates in HD mode. Each SBS is equipped with single antenna and operates in FD mode per channel at one time instant. All the MUs operate in HD mode.

In this work, our study is limited to the DL transmission of macrocells, whereas the UL transmission of macrocells can be studied following the similar approach. The network is assumed to be fully-loaded, such that each MBS has at least U_{M} active MUs, and each SBS serves one active DL MU and one active UL MU. Accordingly, the intensity of the active DL MUs in HCNs is $\lambda_u^{\mathrm{DL}} = (U_{\mathrm{M}}\lambda_{b^{\mathrm{M}}} + \lambda_{b^k})$, whereas the active UL MUs are modeled by an independent HPPP Φ_{u^k} with intensity $\lambda_{u^k}^{\mathrm{UL}} = \lambda_{b^k}$.

The channels are modeled as independent and identically distributed (i.i.d.) quasi-static Rayleigh fading. We assume time division duplexing (TDD) mode, where channel reciprocity can be exploited and allows a MBS to estimate its DL channels from UL pilots sent by the MUs. We consider time division multiple access (TDMA), where several MUs share the same channel in different time slots, thus the BS transmit power is independent of the density of active MUs, and there is no intra-cell interference in each cell. Each MBS transmit U_{M} data streams using linear zero-forcing beamforming (ZFBF) with the equal transmit power allocation [21], thus the uncorrelated intra-cell interference is suppressed. Perfect channel state information (CSI) in the DL and the UL is assumed. In the training phase, each MU sends a pre-assigned orthogonal pilot sequence to the MBS which is estimated perfectly by the MBS and no pilot contamination is assumed.

The MUs use distance-proportional fractional power control [22], in which each MU at a distance d from the associated SBS adjusts its transmit power with $P_u = \rho_k \beta^{-\epsilon} d^{\epsilon\alpha_k}$ to compensate for the large scale fading, where $0 \leq \epsilon \leq 1$ is the UL power control factor and ρ_k is the receiver sensitivity of the kth tier SBSs.

TABLE I
Frequent Notations

Notation	Definition
P_M	Transmit power of MBS
P_k	Transmit power of kth tier SBS
ρ_k	Receiver's sensitivity at the kth tier SBS
ϵ	UL power control factor
α_M	Path loss exponent for Macrocell
α_k	Path loss exponent for kth tier small cell
G_a	Array gain of MBS antenna
β	Frequency dependent constant value
o	Reference node - serving BS for DL/typical MU for UL
b_o^M	MBS at the origin
u_o^M	Macrocell MU at the origin
b_o^k	SBS at the origin
u_o^k	Small cell MU at the origin
$\lvert X_{n_1,n_2}\rvert$	Distance from node n_1 to node n_2, $\{n_1, n_2\} \in \{o, b_o^{\mathrm{M}}, u_o^{\mathrm{M}}, b_o^k, u_o^k\}$
$g_{o,n}$	Small scale fading channel coefficient between node o and node n, $n \in \{b_o^{\mathrm{M}}, u_o^{\mathrm{M}}, b_o^k, u_o^k\}$
h_{n_1,n_2}	Small scale fading channel coefficient between node n_1 and node n_2, $\{n_1, n_2\} \in \{o, b_o^{\mathrm{M}}, u_o^{\mathrm{M}}, b_o^k, u_o^k\}$
N_o	Noise power
$\Gamma(.)$	Gamma function
${}_2F_1[.,.;.;.]$	Gauss hypergeometric function

A. Cell Association Model

To obtain the strongest received signal, we consider the maximum received power cell association rule in the DL transmission of HCNs, where the DL MU connects to the BS which provides the maximum long-term average received power [23]. The average received power at a typical DL MU connected to the MBS m ($m \in \Phi_{b^M}$) is expressed as

$$P_{r,\mathrm{M}} = G_a \frac{P_M}{U_M} \beta |X_{m,u_{\mathrm{M}}}|^{-\alpha_{\mathrm{M}}}, \tag{1}$$

where the array gain G_a of ZFBF transmission is $N - U_{\mathrm{M}} + 1$ [21].

The average received power at a DL MU that is connected to the kth tier SBS b^k ($b^k \in \Phi_{\mathrm{b^k}}$) is expressed as

$$P_{r,b^k} = P_k \beta \left(\left|X_{j,u^k}\right|\right)^{-\alpha_k}. \tag{2}$$

For the UL transmission, the MUs can only associate with the FD SBSs. In [14], it is shown that the HD UL MU should associate to the nearest BS to maximize the mean UL rate. We therefore assume that each MU associates to the nearest SBS.

B. SINR Models

1) DL SINR of a Macrocell MU: The signal-to-interference-plus-noise ratio (SINR) for a typical DL macro-

cell MU u_0^M located at the origin is given as

$$\mathrm{SINR}_{\mathrm{M}}^{\mathrm{DL}} = \frac{P_{\mathrm{M}}\beta\left|X_{o,u_0^{\mathrm{M}}}\right|^{-\alpha_{\mathrm{M}}}}{\underbrace{I_{\mathrm{M},u_0^{\mathrm{M}}} + I_{S,u_0^{\mathrm{M}}} + I_{u_{ul}^s,u_0^{\mathrm{M}}}}_{I_{u_o^{\mathrm{M}}}} + N_0}, \tag{3}$$

where $I_{\mathrm{M},u_0^{\mathrm{M}}}$, $I_{S,u_0^{\mathrm{M}}}$, and $I_{u_{ul}^s,u_0^{\mathrm{M}}}$ are the interferences from other MBSs, SBSs, and UL MUs, respectively, which are given as

$$I_{\mathrm{M},u_0^{\mathrm{M}}} = \sum_{x\in\Phi_b^{\mathrm{M}}} \frac{P_{\mathrm{M}}}{U_{\mathrm{M}}}\beta\left|X_{x,b_0^k}\right|^{-\alpha_{\mathrm{M}}}, \tag{4}$$

$$I_{S,u_0^{\mathrm{M}}} = \sum_{j=2}^{K}\sum_{y\in\Phi_b^j} P_j h_{y,u_o^{\mathrm{M}}}\beta\left|X_{y,u_0^{\mathrm{M}}}\right|^{-\alpha_j}, \tag{5}$$

$$I_{u_{ul}^s,u_0^{\mathrm{M}}} = \sum_{j=2}^{K}\sum_{z\in\Phi_u^j} \rho_j\beta^{-\epsilon}|R_{z,b_z}|^{\epsilon\alpha_j} h_{z,u_0^{\mathrm{M}}}\beta\left|X_{z,u_0^{\mathrm{M}}}\right|^{-\alpha_j}, \tag{6}$$

Note that, the massive MIMO gain, $N - U_{\mathrm{M}} + 1$, and the impact of equal power allocation per backhaul stream (i.e., the denominator of MBS's transmit power $\frac{P_{\mathrm{M}}}{U_{\mathrm{M}}}$) in (3) have been incorporated in the rate coverage probability expression in (19). In (4), there is no short-term fading factor due to channel hardening effect in the interference experienced from the MBSs, whereas, in (5) and (6), $h_{y,u_o^M} \sim \exp(1)$ and $h_{z,u_0^{\mathrm{M}}} \sim \exp(1)$, respectively. In (6), $\rho_j\beta^{-\epsilon}|R_{z,b_z}|^{\epsilon\alpha_j}$is the transmit power of the UL MU at a distance of $|R_{z,b_z}|$from its serving SBS.

2) DL SINR of a Small Cell MU: The SINR for a typical DL small cell MU u_0^k located at the origin can be written as

$$\mathrm{SINR}_k^{\mathrm{DL}} = \frac{P_k g_{o,u_0^k}\beta\left|X_{o,u_0^k}\right|^{-\alpha_k}}{I_{\mathrm{M},u_0^k} + I_{S,u_0^k} + I_{u_{ul}^s,u_0^k} + N_0}, \tag{7}$$

where I_{M,u_0^k} , I_{S,u_0^k} , and $I_{u_{ul}^s,u_0^k}$ are the interferences from MBSs, other SBSs, and UL MUs, respectively, which are given as

$$I_{\mathrm{M},u_0^k} = \sum_{x\in\Phi_b^{\mathrm{M}}} \frac{P_{\mathrm{M}}}{U_{\mathrm{M}}}\beta\left|X_{x,u_0^k}\right|^{-\alpha_{\mathrm{M}}}, \tag{8}$$

$$I_{S,u_0^k} = \sum_{j=2}^{K}\sum_{y\in\Phi_b^j\setminus o} P_j h_{y,u_0^k}\beta\left|X_{y,u_0^k}\right|^{-\alpha_j}, \tag{9}$$

and

$$I_{u_{ul}^s,u_0^k} = \sum_{j=2}^{K}\sum_{z\in\Phi_u^j} \rho_j\beta^{-\epsilon}|R_{z,b_z}|^{\epsilon\alpha_j} h_{z,u_0^k}\beta\left|X_{z,u_0^k}\right|^{-\alpha_j}. \tag{10}$$

3) UL SINR of a Small Cell MU: The UL SINR for a typical SBS b_0^k located at the origin can be written as

$$\mathrm{SINR}_k^{\mathrm{UL}} = \frac{\rho_k g_{o,b_0^k}\beta^{(1-\epsilon)}\left|X_{o,b_0^k}\right|^{\alpha_k(\epsilon-1)}}{P_k h_{LI} + I_{\mathrm{M},b_0^k} + I_{S,b_0^k} + I_{u_{ul}^s,b_0^k} + N_0}, \tag{11}$$

where $P_k h_{LI}$ is the residual SI power after performing cancellation. We define $P_k h_{LI} = P_k \,.\, 10^{L_{dB,k}/10}$, and $L_{dB,k}$ is the ratio of the residual self-interference after interference cancellation to the transmission power at the kth tier BS as defined in [13]. In (11), I_{M,b_0^k} , I_{S,b_0^k} , and $I_{u_{ul}^s,b_0^k}$ are the interferences from MBSs, SBSs, and the other UL MUs, respectively, which are given as

$$I_{\mathrm{M},b_0^k} = \sum_{x\in\Phi_b^{\mathrm{M}}} \frac{P_{\mathrm{M}}}{U_{\mathrm{M}}}\beta\left|X_{x,b_0^k}\right|^{-\alpha_{\mathrm{M}}}, \tag{12}$$

$$I_{S,b_0^k} = \sum_{j=2}^{K}\sum_{y\in\Phi_b^j\setminus b_0^k} P_j h_{y,b_0^k}\beta\left|X_{y,b_0^k}\right|^{-\alpha_j}, \tag{13}$$

and

$$I_{u_{ul}^s,b_0^k} = \sum_{j=2}^{K}\sum_{z\in\Phi_u^j\setminus o} \rho_j\beta^{-\epsilon}|R_{z,b_z}|^{\epsilon\alpha_j} h_{z,b_0^k}\beta\left|X_{z,b_0^k}\right|^{-\alpha_j}. \tag{14}$$

III. Performance Evaluation

In this section, we characterize the performance of K tier HCNs in terms of the DL and UL rate coverage probability. The rate coverage probability is defined as the probability of DL (UL) transmission rate to be higher than a required rate threshold R^{DL} (R^{UL}) for a given link. To facilitate the analysis, we first present per tier association probability [24].

A. DL Cell Association

The probability that a typical MU is associated with the MBS is given as

$$\Lambda_{\mathrm{M}} = 2\pi\lambda_{b^{\mathrm{M}}}\int_0^\infty r\exp\Bigg\{-\pi\lambda_{b^{\mathrm{M}}}r^2 - \pi\sum_{j=2}^{K}\lambda_{b^k}\left(\frac{P_j U_{\mathrm{M}}}{(N-U_{\mathrm{M}}+1)P_{\mathrm{M}}}\right)^{2/\alpha_j} r^{2\alpha_{\mathrm{M}}/\alpha_j}\Bigg\}\mathrm{d}r. \tag{15}$$

The probability that a typical MU is associated with the kth tier SBS is given as

$$\Lambda_k^{\mathrm{DL}} = 2\pi\lambda_{b^k}\int_0^\infty r\exp\Bigg\{-\pi\sum_{j=2}^{K}\lambda_{b^j}(P_j r^{\alpha_k}/P_k)^{2/\alpha_j} - \pi\lambda_{b^{\mathrm{M}}}\left(\frac{P_{\mathrm{M}}(N-U_{\mathrm{M}}+1)}{P_k U_{\mathrm{M}}}\right)^{2/\alpha_{\mathrm{M}}} r^{2\alpha_k/\alpha_{\mathrm{M}}}\Bigg\}\mathrm{d}r. \tag{16}$$

B. UL Cell Association

In the UL transmission, a typical MUs can only associate with the nearest FD SBS. The probability that a typical MU is associated with the kth tier SBS is defined as

$$\Lambda_k^{\mathrm{UL}} = 2\pi\lambda_{b^k}\int_0^\infty r\exp\Big\{-\sum_{j=2}^{K}\pi\lambda_j r^{2\alpha_k/\alpha_j}\Big\}\mathrm{d}r. \tag{17}$$

C. DL Rate Coverage Probability

In this section, we derive the DL rate coverage probability of a typical MU in the K-tier HCNs. The DL rate coverage probability of a random MU in the K-tier HCNs is given by

$$C^{DL}(\mathrm{R}^{\mathrm{DL}}) = \Lambda_{\mathrm{M}} C_{\mathrm{M}}(\mathrm{R}^{\mathrm{DL}}) + \sum_{k=2}^{K}\Lambda_k^{\mathrm{DL}} C_k^{\mathrm{DL}}(\mathrm{R}^{\mathrm{DL}}), \tag{18}$$

where Λ_{M} and Λ_k^{DL} are given in (15) and (16), respectively, $C_{\mathrm{M}}(\mathrm{R}^{\mathrm{DL}})$ is the DL rate coverage probability between a typical MU and its serving MBS, and $C_k^{\mathrm{DL}}(\mathrm{R}^{\mathrm{DL}})$ is the DL

rate coverage probability between a typical MU and its serving SBS.

In (18), the DL rate coverage probability between a typical MU and its serving MBS is defined as

$$C_M(\mathrm{R^{DL}}) = \mathbb{E}_{\left|X_{o,u_0^{\mathrm{M}}}\right|}\Big[\mathbb{E}_{\mathrm{SINR_M^{DL}}}\Big[\Pr\Big[\mathrm{SINR_M^{DL}}\left(\left|X_{o,u_0^{\mathrm{M}}}\right|\right) \geq \gamma_{\mathrm{M}}\Big]\Big]\Big], \tag{19}$$

where $\mathrm{SINR_M^{DL}}$ is given in (3) and γ_{M} is given as

$$\gamma_{\mathrm{M}} = \frac{U_{\mathrm{M}}}{N - U_{\mathrm{M}} + 1}\left(\mathrm{e}^{\mathrm{R^{DL}}} - 1\right), \tag{20}$$

where $\mathrm{R^{DL}}$is the DL rate threshold. Similarly, the DL rate coverage probability of typical MU at a distance $\left|X_{o,u_0^k}\right|$from its associated SBS in the kth tier is defined as

$$C_k^{\mathrm{DL}}(\mathrm{R^{DL}}) = \mathbb{E}_{\left|X_{o,u_0^k}\right|}\Big[\Pr\Big[\mathrm{SINR_k^{DL}}\left(\left|X_{o,u_0^k}\right|\right) \geq \gamma_S^{\mathrm{DL}}\Big]\Big], \tag{21}$$

where $\mathrm{SINR_k^{DL}}$is given in (7), and $\gamma_S^{\mathrm{DL}}$is given as.

$$\gamma_S^{\mathrm{DL}} = \mathrm{e}^{\mathrm{R^{DL}}} - 1. \tag{22}$$

Theorem 1. *The DL rate coverage probability of a typical MU associated with the MBS is derived as*

$$C_{\mathrm{M}}(\mathrm{R^{DL}}) = \frac{2\pi\lambda_{\mathrm{b^M}}}{\Lambda_{\mathrm{M}}}\int_0^\infty x\Bigg[\frac{1}{2} - \frac{1}{\pi}\int_0^\infty \mathrm{Im}\Big[\exp\Big\{-\chi_1(x,\mathrm{w}) - \pi\lambda_{b^{\mathrm{M}}}\chi_2(x,\mathrm{w}) - \chi_3(x,\mathrm{w}) - \chi_4(x,\mathrm{w}) - \pi\lambda_{\mathrm{b^M}}x^2 - \pi\sum_{j=2}^{K}\lambda_{\mathrm{b^k}}\left(\frac{P_jU_{\mathrm{M}}}{(N-U_{\mathrm{M}}+1)P_{\mathrm{M}}}\right)^{2/\alpha_j} r^{2\alpha_{\mathrm{M}}/\alpha_j}\Big\}\Big]\Bigg]\frac{\mathrm{dw}}{\mathrm{w}}\,\mathrm{d}x, \tag{23}$$

where

$$\chi_1(x,\mathrm{w}) = \mathrm{jw}\left(\frac{P_{\mathrm{M}}\beta}{\gamma_{\mathrm{M}}x^{\alpha_{\mathrm{M}}}} - N_o\right), \tag{24}$$

$$\chi_2(x,\mathrm{w}) = \frac{\Gamma\left(1-\frac{2}{\alpha_{\mathrm{M}}}\right) + \frac{2}{\alpha_{\mathrm{M}}}\Gamma_u\left(-\frac{2}{\alpha_{\mathrm{M}}}, \frac{-\mathrm{jw}P_{\mathrm{M}}\beta}{x^{\alpha_{\mathrm{M}}}}\right)}{(-\mathrm{jw}P_{\mathrm{M}}\beta)^{\frac{2}{\alpha_{\mathrm{M}}}}} - x^2, \tag{25}$$

$$\chi_3(x,\mathrm{w}) = \sum_{j=2}^{K} 2\pi\lambda_{bj}\left(\frac{{P_j}^{\alpha_j/2}(-\mathrm{jw})\beta(\frac{x^{\alpha_{\mathrm{M}}}U_{\mathrm{M}}}{(N-U_{\mathrm{M}}+1)P_{\mathrm{M}}})^{2/\alpha_j-1}}{\alpha_j - 2}\right) {}_2F_1\left[1, 1-\frac{2}{\alpha_j}; 2-\frac{2}{\alpha_j}; \frac{\mathrm{jw}(N-U_{\mathrm{M}}+1)P_{\mathrm{M}}}{U_{\mathrm{M}}x^{\alpha_{\mathrm{M}}}}\right], \tag{26}$$

$$\chi_4(x,\mathrm{w}) = \int_0^\infty\int_0^{r^2}\frac{\left(\pi\sum\limits_{j=2}^{K}\lambda_{bj}e^{-\pi\sum\limits_{j=2}^{K}\lambda_{bj}u}\right)\lambda_{I_{\Phi_{bj}^{\mathrm{UL}}}}(r)}{1+(-\mathrm{jw}\rho_j\beta^{(1-\epsilon)})^{-1}u^{-\alpha_j\epsilon/2}r^{\alpha_j}}\,\mathrm{d}u\,r\mathrm{d}r, \tag{27}$$

and Λ_{M}*,* γ_{M}*, and* $\lambda_{I_{\Phi_{bj}^{\mathrm{UL}}}}(r)$*are given in* (15)*,* (20)*, and* (A.6)*, respectively.*

Proof. See Appendix A. □

Theorem 2. *The DL rate coverage probability of a typical MU associated with the kth tier SBS is derived as*

$$C_k^{\mathrm{DL}}(\mathrm{R^{DL}}) = \frac{2\pi\lambda_{\mathrm{b^k}}}{\Lambda_{\mathrm{k}}^{\mathrm{DL}}}\int_0^\infty x\Bigg[\frac{1}{2} - \frac{1}{\pi}\int_0^\infty \mathrm{Im}\Big[\exp\Big\{\mathrm{jw}N_o - \pi\lambda_{b^{\mathrm{M}}}\varpi_1(x,\mathrm{w}) - \varpi_2(x,\mathrm{w}) - \varpi_3(x,\mathrm{w}) - \pi\sum_{j=2}^{K}\lambda_{\mathrm{bj}}\left(\frac{P_jx^{\alpha_{\mathrm{k}}}}{P_k}\right)^{\frac{2}{\alpha_{\mathrm{j}}}} - \pi\lambda_{\mathrm{b^M}}x^{\frac{2\alpha_{\mathrm{k}}}{\alpha_{\mathrm{M}}}}\left(\frac{P_{\mathrm{M}}(N-U_{\mathrm{M}}+1)}{U_{\mathrm{M}}P_{\mathrm{k}}}\right)^{\frac{2}{\alpha_{\mathrm{M}}}}\Big\}\left(1+\frac{\mathrm{jw}P_k\beta}{\gamma_S^{DL}x^{\alpha_k}}\right)^{-1}\Big]\Bigg]\frac{\mathrm{dw}}{\mathrm{w}}\,\mathrm{d}x, \tag{28}$$

where

$$\varpi_1(x,\mathrm{w}) = \frac{\Gamma\left(1-\frac{2}{\alpha_{\mathrm{M}}}\right) + \frac{2}{\alpha_{\mathrm{M}}}\Gamma_u\left(-\frac{2}{\alpha_{\mathrm{M}}}, \frac{-\mathrm{jw}P_M\beta}{(D_k^{\mathrm{M}}(x))^{\alpha_{\mathrm{M}}}}\right)}{(-\mathrm{jw}P_{\mathrm{M}}\beta)^{\frac{2}{\alpha_{\mathrm{M}}}}} - \left(D_k^{\mathrm{M}}(x)\right)^2, \tag{29}$$

$$\varpi_2(x,\mathrm{w}) = \left(\frac{\left(\frac{P_j}{P_k}\right)^{2/\alpha_j}(-\mathrm{jw})\beta P_k(x^{\alpha_k})^{2/\alpha_j-1}}{\alpha_j - 2}\right) {}_2F_1\left[1, 1-\frac{2}{\alpha_j}; 2-\frac{2}{\alpha_j}; \frac{\mathrm{jw}\beta P_j}{x^{\alpha_k}}\left(D_j^k(x)\right)^{\alpha_k-\alpha_j}\right], \tag{30}$$

$$\varpi_3(x,\mathrm{w}) = \int_0^\infty\int_0^{r^2}\frac{\left(\pi\sum\limits_{j=2}^{K}\lambda_{bj}e^{-\pi\sum\limits_{j=2}^{K}\lambda_{bj}u}\right)\lambda_{I_{\Phi_{bj}^{\mathrm{UL}}}}(r)}{1+(-\mathrm{jw}\rho_j\beta^{(1-\epsilon)})^{-1}u^{-\alpha_j\epsilon/2}r^{\alpha_j}}\,\mathrm{d}u\,r\mathrm{d}r, \tag{31}$$

$D_k^{\mathrm{M}}(x) = \left(\frac{(N-U_{\mathrm{M}}+1)P_{\mathrm{M}}}{U_{\mathrm{M}}P_k}\right)^{\frac{1}{\alpha_{\mathrm{M}}}}x^{\frac{\alpha_k}{\alpha_{\mathrm{M}}}}$ *is the distance between the closest interfering MBS and the typical MU,* $D_j^k(x) = \left(\frac{P_j}{P_k}\right)^{\frac{1}{\alpha_j}}x^{\frac{\alpha_k}{\alpha_j}}$ *is the distance between the closest interfering BS in the* j*th tier and the typical MU, and* $\lambda_{I_{\Phi_{bj}^{\mathrm{UL}}}}(r)$ *is given in* (A.6)*. In* (28)*,* $\Lambda_{\mathrm{k}}^{\mathrm{DL}}$*and* γ_S^{DL}*are given in* (16) *and* (22)*, respectively.*

Proof. The proof follows analogous steps to Theorem 1. □

D. UL Rate Coverage Probability

In this section, we derive the UL rate coverage probability using

$$C^{\mathrm{UL}}(\mathrm{R^{UL}}) = \sum_{k=2}^{K}\Lambda_k^{\mathrm{UL}}C_k^{\mathrm{UL}}(\mathrm{R^{UL}}), \tag{32}$$

where $\Lambda_k^{\mathrm{UL}}$is given in (17), and $C_k^{\mathrm{UL}}$is the UL rate coverage probability between a typical MU and its serving SBS defined as

$$C_k^{\mathrm{UL}}(\mathrm{R^{UL}}) = \mathbb{E}_{\left|X_{o,b_0^k}\right|}\Big[\Pr\Big[\mathrm{SINR_k^{UL}}\left(\left|X_{o,b_0^k}\right|\right) \geq \gamma_S^{\mathrm{UL}}\Big]\Big]. \tag{33}$$

where $\mathrm{SINR_k^{UL}}$is given in (11) and γ_S^{UL} is given as

$$\gamma_S^{\mathrm{UL}} = \mathrm{e}^{\mathrm{R^{UL}}} - 1, \tag{34}$$

where $\mathrm{R^{UL}}$is the UL rate threshold.

Theorem 3. *The UL rate coverage probability of a typical MU associated with the kth tier SBS is derived as*

$$C_k^{\mathrm{UL}}(\mathrm{R}^{\mathrm{UL}}) = \frac{2\pi\lambda_{\mathrm{b^K}}}{\Lambda_{\mathrm{k}}^{\mathrm{UL}}} \int_0^{\infty} x \left[\frac{1}{2} - \frac{1}{\pi} \int_0^{\infty} \mathrm{Im} \left[\exp\left\{ \mathrm{j}\mathrm{w} N_o - \pi\lambda_{b^{\mathrm{M}}} \vartheta_1(x,\mathrm{w}) - \vartheta_2(x,\mathrm{w}) - \vartheta_3(x,\mathrm{w}) - \sum_{j=2}^{K} \pi\lambda_{b^j} x^{\frac{2\alpha_k}{\alpha_j}} \right\} \left(1 + \frac{\mathrm{j}\mathrm{w}\rho_k x^{\alpha_k \epsilon} \beta^{-\epsilon} \beta}{\gamma_S^{UL} x^{\alpha_k}} \right)^{-1} \right] \right] \frac{\mathrm{d}\mathrm{w}}{\mathrm{w}} \, \mathrm{d}x, \tag{35}$$

where

$$\vartheta_1(x,\mathrm{w}) = (-\mathrm{j}\mathrm{w} P_{\mathrm{M}} \beta)^{\frac{2}{\alpha_{\mathrm{M}}}} \Gamma\left(1 - \frac{2}{\alpha_{\mathrm{M}}}\right), \tag{36}$$

$$\vartheta_2(x,\mathrm{w}) = (-\mathrm{j}\mathrm{w} P_j \beta) \frac{x^{2-\alpha_j}}{(\alpha_j - 2)} \, {}_2F_1\left[1, 1 - \frac{2}{\alpha_j}; 2 - \frac{2}{\alpha_j}; \frac{\mathrm{j}\mathrm{w}\beta P_j}{x^{\alpha_k}} x^{(\alpha_k - \alpha_j)}\right], \tag{37}$$

$$\vartheta_3(x,\mathrm{w}) = \int_0^{\infty} \int_0^{r^2} \frac{\left(\pi \sum_{j=2}^{K} \lambda_{b^j} e^{-\pi \sum_{j=2}^{K} \lambda_{b^j} u} \right)}{1 + \left(-\mathrm{j}\mathrm{w}\rho_j \beta^{1-\epsilon}\right)^{-1} u^{-\alpha_j \epsilon/2} r^{\alpha_j}} \, \mathrm{d}u \, r \mathrm{d}r, \tag{38}$$

and $\Lambda_{\mathrm{k}}^{\mathrm{UL}}$ *and* γ_S^{UL} *are given in* (17) *and* (34)*, respectively.*

Proof. The proof follows analogous steps to Theorem 1. □

IV. Numerical Results

In this section, we investigate the DL and UL rate coverage probability in massive MIMO enabled HCNs with FD small cells. We plot the DL rate coverage probability of macrocell MU, small cell MU and a random MU in HCNs using (23), (28), and (18), respectively. We plot the UL rate coverage probability of small cell MU using (35). We validate the accuracy of the derived expressions for a two-tier HCN consisting of macrocells with density $\lambda_{b^{\mathrm{M}}} = 5 \times 10^{-5}$ and small cells with density λ_{b^2}. Unless specified, the transmit powers at the MBSs and SBSs are 40 dBm and 30 dBm, respectively. For all the numerical analysis, thermal noise is set as $N_0 = -100$ dBm for 10 MHz bandwidth and the DL and the UL rate thresholds are taken to be equal $\mathrm{R}^{\mathrm{DL}} = \mathrm{R}^{\mathrm{UL}}$.

In Fig. 1, we examine the rate coverage probability of the proposed HCNs versus the ratio between density of SBSs to density of MBS ($\mu = \lambda_{b^2}/\lambda_{b^{\mathrm{M}}}$) for different values of number of antennas at MBSs N. The increase in λ_{b^2}, improves the DL rate coverage probabilities of macrocell MU and small cell MU. This is due to the fact that increasing λ_{b^2} decreases the distance between the typical small cell MU and the serving SBS. Thus, the MUs transmit with less power due to distance-proportional fractional power control which reduces the UL interference. However, increasing λ_{b^2} decreases the UL rate coverage probability due to the increased interference from the larger number of SBSs. The DL rate coverage probability of macrocell MU and small cell MU are increased at higher N due to the large antenna array gain. However, the UL rate coverage of MU remains constant with increasing N due to the facts that the UL MU can only associate with the small cell and the interference from the MBSs to the UL MU relatively small.

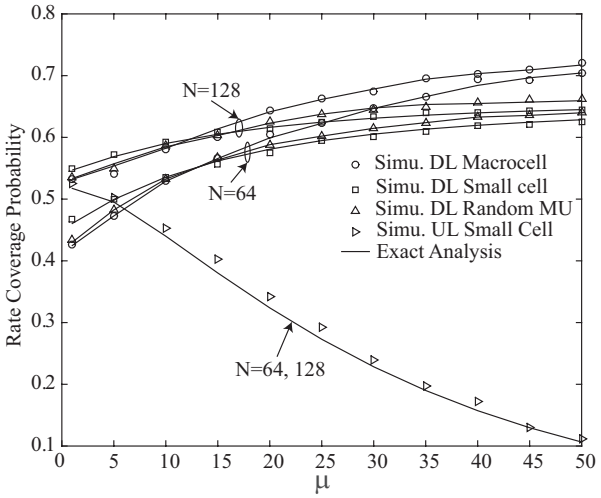

Fig. 1. Impact of SBS density with different number of MIMO antennas at MBS in a two-tier HCNs with parameters $\{\alpha_{\mathrm{M}}, \alpha_2\} = \{3.5, 4\}, U_{\mathrm{M}} = 5, \rho_2 = -40$ dBm, $\epsilon = 0.9$, and $P_k h_{LI} = 0$.

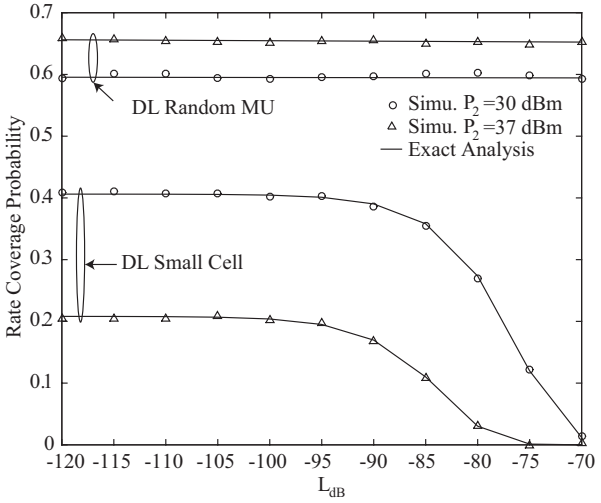

Fig. 2. Impact of SI cancellation capability with different SBSs transmit power in a two-tier HCNs with parameters $\mu = 20\,\{\alpha_{\mathrm{M}}, \alpha_2\} = \{3.5, 4\}$, $N = 128$, $U_{\mathrm{M}} = 5$, $\rho_2 = -40$ dBm, and $\epsilon = 0.9$.

Fig. 2 examines the impact of the SI cancellation capability L_{dB} on the DL and UL rate coverage probabilities. As expected, increasing L_{dB} decreases the UL rate coverage probability of the small cell MU. Moreover, increasing the SBS transmit power decreases the UL rate coverage probability of the small cell MU, due to the increased self interference. However, increasing the SBS transmit power increases the DL rate coverage probability of a random MU, due to the increase of $\mathrm{SINR}_{\mathrm{k}}^{\mathrm{DL}}$ in (7).

Fig. 3 plots the DL and UL rate coverage probability versus

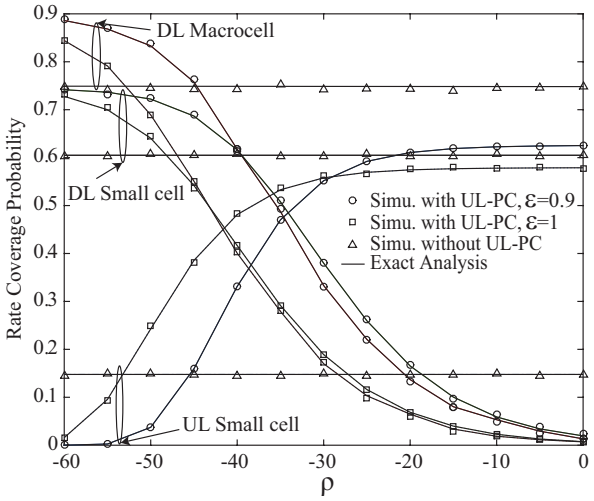

Fig. 3. Impact of SBS receiver sensitivity with different power control factors in a two-tier HCNs with parameters $\mu = 20\,\{\alpha_{\rm M}, \alpha_2\} = \{3.5, 4\}$, $N = 128$, $U_{\rm M} = 5$, and $P_k h_{LI} = 0$.

receiver's sensitivity at SBSs ρ_2 for different values of power control factors ϵ. It also compares the DL and UL performance of HCNs with UL power control to that without UL power control with MUs transmit power $P_u = 23$ dBm. The UL rate coverage improves while the DL rate coverage degrades with the increase of ρ_2. This is due to the reason that a decrease in the the SBS receiver sensitivity (i.e., an increase in ρ_2) increases the transmit power required by each MU to perform channel inversion towards serving SBS, which in turn increases the useful signal at the serving SBS and the interference at the other BSs and MUs. Similarly, higher power control factor ϵ improves the UL performance while degrades the DL performance. These results show the need of an appropriate selection of ρ_2 and ϵ for joint DL and UL performance gain. On the contrary, the UL rate coverage probability in HCNs without UL power control is shown to be very small due to the increased inter-cell interference from the UL MUs.

V. Conclusions

In this paper, we have presented a tractable model for massive MIMO enabled HCNs with FD small cells. Relying on stochastic geometry, we have derived the analytical expressions for the DL rate coverage probabilities for the macrocell MUs and small cell MUs, and the UL rate coverage probability for small cell MUs. It is shown that the DL rate coverage probability of the network improves with large number of antennas equipped at the MBSs. We have shown that increasing the SBSs density increases the DL rate coverage probability but decreases the UL rate coverage probability, therefore, can be used to achieve either a better DL rate coverage probability at the cost of lower UL coverage probability or vice versa. Our results also demonstrate the joint gain on the DL and the UL rate coverage probabilities by using the UL fractional power control.

Appendix A
Proof of Theorem 1

Based on (3), the DL rate coverage probability of the macrocell tier with massive MIMO at the BSs, can be given as

$$C_{\rm M}(\mathrm{R_{DL}}) = \int_0^\infty F_{I_{u_0^{\rm M}}}\left(\frac{P_{\rm M}\beta}{\gamma_{\rm M}|X_{o,u_0^{\rm M}}|^{\alpha_{\rm M}}} - N_o\right) f_{|X_{o,{\rm M}}|}(x)\,\mathrm{d}x, \tag{A.1}$$

where $f_{|X_{o,{\rm M}}|}(x)$is the PDF of the distance between a typical MU and its serving BS given by [24]. In (A.1), we resort to apply the Gil-Pelaez inversion theorem and the CDF of the interference $F_{I_{u_0^{\rm M}}}(.)$can be derived as

$$\begin{aligned} &F_{I_{u_0^{\rm M}}}(x) \\ =&\frac{1}{2} - \frac{1}{\pi}\int_0^\infty \mathrm{Im}\left[\frac{\mathcal{L}_{I_{{\rm M},u_0^k}}(-\mathrm{jw})\mathcal{L}_{I_{S,u_0^k}}(-\mathrm{jw})\mathcal{L}_{I_{u_{ul}^s,u_0^k}}(-\mathrm{jw})}{\exp\left(\mathrm{jw}\left(\frac{P_{\rm M}\beta}{\gamma x^{\alpha_{\rm M}}} - N_o\right)\right)}\right]\frac{\mathrm{dw}}{\mathrm{w}}, \end{aligned} \tag{A.2}$$

where $\mathrm{Im}(.)$ represents the imaginary part of the argument. In (A.2), the Laplace transform of $I_{{\rm M},u_0^k}$can be derived as under

$$\begin{aligned} &\mathcal{L}_{I_{{\rm M},u_0^k}}(-\mathrm{jw}) \\ &\overset{(a)}{=} \exp\left\{-2\pi\lambda_{b^{\rm M}}\int_x^\infty \left(1 - \exp\{-(-\mathrm{jw})P_{\rm M}\beta r^{\alpha_{\rm M}}\}\right) r dr\right\} \\ &\overset{(b)}{=} \exp\left\{-\pi\lambda_{b^{\rm M}}\left(\frac{\Gamma\left(1-\frac{2}{\alpha_{\rm M}}\right) + \frac{2}{\alpha_{\rm M}}\Gamma_u\left(-\frac{2}{\alpha_{\rm M}}, \frac{-\mathrm{jw}P_{\rm M}\beta}{x^{\alpha_{\rm M}}}\right)}{(-\mathrm{jw}P_{\rm M}\beta)^{\frac{2}{\alpha_{\rm M}}}} - x^2\right)\right\}, \end{aligned} \tag{A.3}$$

where (a) follows from the probability generating functional of PPP and (b) follows from solving integral in (a). Similarly, following (A.3), the Laplace transform of I_{S,u_0^k}can be evaluated as

$$\mathcal{L}_{I_{S,u_0^k}}(-\mathrm{jw}) = \exp\left\{-\sum_{j=2}^K 2\pi\lambda_{b^j}\int_{D_j^{\rm M}(x)}^\infty \left(\frac{-\mathrm{jw}P_j\beta r^{-\alpha_j}}{1-\mathrm{jw}P_j\beta r^{-\alpha_j}}\right) r\mathrm{d}r\right\}, \tag{A.4}$$

where $D_j^{\rm M}(x) = \left(\frac{P_j U_{\rm M}}{(N-U_{\rm M}+1)P_{\rm M}}\right)^{\frac{1}{\alpha_j}} x^{\frac{\alpha_{\rm M}}{\alpha_j}}$ is the distance between the closest interfering BS in the jth tier and the typical macrocell MU. Likewise, the Laplace transform of $I_{u_{ul}^s,u_0^k}$ is obtained as

$$\mathcal{L}_{I_{u_{ul}^s,u_0^k}}(-\mathrm{jw}) \overset{(a)}{=} \exp\left\{-\sum_{j=2}^K 2\pi\lambda_{b^j}\int_0^\infty \lambda_{I_{\Phi_{b^j}^{\rm UL}}}(r)\,\mathbb{E}_R\left[\frac{-\mathrm{jw}\rho_j\beta^{1-\epsilon}R^{\epsilon\alpha_j}r^{-\alpha_j}}{1-\mathrm{jw}\rho_j\beta^{1-\epsilon}R^{\epsilon\alpha_j}r^{-\alpha_j}}\right] r\mathrm{d}r\right\}, \tag{A.5}$$

where (a) follows from the probability generating functional of a PPP and the fact that the UL interference field is a non-homogeneous PPP with distance dependent density function given as

$$\lambda_{I_{\Phi_{b^j}^{\mathrm{UL}}}}(r) = \lambda_{b^j}(1 - \exp(-\pi \frac{\lambda_{b^j}}{A_j^{UL}} r^2)) \qquad \text{(A.6)}$$

where $(A_j^{UL} = \lambda_{b^j} / \sum_{i=2}^{K} \lambda_{b^i})$ is the repulsion parameter as in [25]. Using the PDF of serving link distances R in [26], we derive $\mathcal{L}_{I_{u_{ul}^s, u_0^k}}(-\mathrm{jw})$. Substituting (A.3), (A.4), and (A.5) into (A.2), and finally plugging (A.2) into (A.1), we obtain Theorem 1.

REFERENCES

[1] J. Andrews, S. Buzzi, W. Choi, S. Hanly, A. Lozano, A. Soong, and J. Zhang, "What will 5G be?" *IEEE J. Sel. Areas Commun.*, vol. 32, no. 6, pp. 1065–1082, Jun. 2014.

[2] K. N. R. S. V. Prasad, E. Hossain, and V. K. Bhargava, "Energy efficiency in massive MIMO-based 5G networks: Opportunities and challenges," *IEEE Trans. Commun.*, to appear.

[3] C. X. Wang, F. Haider, X. Gao, X. H. You, Y. Yang, D. Yuan, H. M. Aggoune, H. Haas, S. Fletcher, and E. Hepsaydir, "Cellular architecture and key technologies for 5G wireless communication networks," *IEEE Commun. Mag.*, vol. 52, no. 2, pp. 122–130, Feb. 2014.

[4] V. Jungnickel, K. Manolakis, W. Zirwas, B. Panzner, V. Braun, M. Lossow, M. Sternad, R. Apelfrojd, and T. Svensson, "The role of small cells, coordinated multipoint, and massive MIMO in 5G," *IEEE Commun. Mag.*, vol. 52, no. 5, pp. 44–51, May 2014.

[5] S. Parkvall, A. Furuskar, and E. Dahlman, "Evolution of lte toward imt-advanced," *IEEE Commun. Mag.*, vol. 49, no. 2, pp. 84–91, Feb. 2011.

[6] H. Q. Ngo, E. G. Larsson, and T. L. Marzetta, "Energy and spectral efficiency of very large multiuser MIMO systems," *IEEE Trans. Commun.*, vol. 61, no. 4, pp. 1436–1449, Apr. 2013.

[7] A. Sabharwal, P. Schniter, D. Guo, D. W. Bliss, S. Rangarajan, and R. Wichman, "In-band full-duplex wireless: Challenges and opportunities," *IEEE J. Sel. Areas Commun.*, vol. 32, no. 9, pp. 1637–1652, Sept. 2014.

[8] T. Snow, C. Fulton, and W. J. Chappell, "Transmit-receive duplexing using digital beamforming system to cancel self-interference," *IEEE Trans. Microw. Theory Tech.*, vol. 59, no. 12, pp. 3494–3503, Dec. 2011.

[9] T. Riihonen, S. Werner, and R. Wichman, "Mitigation of loopback self-interference in full-duplex MIMO relays," *IEEE Trans. Signal Process.*, vol. 59, no. 12, pp. 5983–5993, Dec. 2011.

[10] H. Alves, C. H. M. de Lima, P. H. J. Nardelli, R. D. Souza, and M. Latva-aho, "On the average spectral efficiency of interference-limited full-duplex networks," in *2014 9th International Conference on Cognitive Radio Oriented Wireless Networks and Communications (CROWNCOM)*, June 2014, pp. 550–554.

[11] S. Goyal, C. Galiotto, N. Marchetti, and S. Panwar, "Throughput and coverage for a mixed full and half duplex small cell network," in *2016 IEEE International Conference on Communications (ICC)*, May 2016, pp. 1–7.

[12] H. Tabassum, A. H. Sakr, and E. Hossain, "Massive MIMO-enabled wireless backhauls for full-duplex small cells," in *Proc. IEEE GLOBECOM*, Dec. 2015, pp. 1–6.

[13] J. Lee and T. Q. S. Quek, "Hybrid full-/half-duplex system analysis in heterogeneous wireless networks," *IEEE Trans. Wireless Commun.*, vol. 14, no. 5, pp. 2883–2895, May. 2015.

[14] A. H. Sakr and E. Hossain, "On cell association in multi-tier full-duplex cellular networks," *CoRR*, vol. abs/1607.01119, 2016. [Online]. Available: http://arxiv.org/abs/1607.01119

[15] M. Naslcheraghi, S. A. Ghorashi, and M. Shikh-Bahaei, "FD device-to-device communication for wireless video distribution," *IET Communications*, vol. 11, no. 7, pp. 1074–1081, 2017.

[16] M. O. Al-Kadri, Y. Deng, A. Aijaz, and A. Nallanathan, "Full-duplex small cells for next generation heterogeneous cellular networks: A case study of outage and rate coverage analysis," *IEEE Access*, vol. 5, pp. 8025–8038, 2017.

[17] A. AlAmmouri, H. ElSawy, O. Amin, and M. S. Alouini, "In-band α -duplex scheme for cellular networks: A stochastic geometry approach," *IEEE Trans. Wireless Commun.*, vol. 15, no. 10, pp. 6797–6812, Oct. 2016.

[18] J. Hoydis, K. Hosseini, S. T. Brink, and M. Debbah, "Making smart use of excess antennas: Massive MIMO, small cells, and TDD," *Bell Labs Technical Journal*, vol. 18, no. 2, pp. 5–21, Sep. 2013.

[19] S. Akbar, Y. Deng, A. Nallanathan, M. Elkashlan, and A. H. Aghvami, "Simultaneous wireless information and power transfer in k -tier heterogeneous cellular networks," *IEEE Transactions on Wireless Communications*, vol. 15, no. 8, pp. 5804–5818, Aug 2016.

[20] Y. Deng, L. Wang, M. Elkashlan, M. D. Renzo, and J. Yuan, "Modeling and analysis of wireless power transfer in heterogeneous cellular networks," *IEEE Transactions on Communications*, vol. 64, no. 12, pp. 5290–5303, Dec 2016.

[21] K. Hosseini, W. Yu, and R. S. Adve, "Large-scale MIMO versus network MIMO for multicell interference mitigation," *IEEE J. Sel. Areas Commun.*, vol. 8, no. 5, pp. 930–941, Oct. 2014.

[22] T. D. Novlan, H. S. Dhillon, and J. G. Andrews, "Analytical modeling of uplink cellular networks," *IEEE Trans. Wireless Commun.*, vol. 12, no. 6, pp. 2669–2679, June 2013.

[23] H.-S. Jo, Y. J. Sang, P. Xia, and J. G. Andrews, "Heterogeneous cellular networks with flexible cell association: A comprehensive downlink SINR analysis," *IEEE Trans. Wireless Commun.*, vol. 11, no. 10, pp. 3484–3495, Oct. 2012.

[24] A. He, L. Wang, Y. Chen, M. Elkashlan, and K. K. Wong, "Massive MIMO in K-tier heterogeneous cellular networks: Coverage and rate," in *2015 IEEE Global Communications Conference (GLOBECOM)*, Dec. 2015, pp. 1–6.

[25] S. Singh, X. Zhang, and J. G. Andrews, "Joint rate and SINR coverage analysis for decoupled uplink-downlink biased cell associations in hetnets," *IEEE Trans. Wireless Commun.*, vol. 14, no. 10, pp. 5360–5373, Oct 2015.

[26] J. G. Andrews, A. K. Gupta, and H. S. Dhillon, "A primer on cellular network analysis using stochastic geometry," *CoRR*, vol. abs/1604.03183, 2016. [Online]. Available: http://arxiv.org/abs/1604.03183